

# Dynamic adsorption behaviors of $\text{Pb}^{2+}$ under complex conditions in lab-scale continuous biochar fixed-bed system: breakthrough curve characteristics and parameters

Ji Zehua Pei Yuansheng \*

(The Key Laboratory of Water and Sediment Sciences, Ministry of Education, School of Environment, Beijing Normal University, No. 19, Xijiekouwai Street, Beijing 100875, China)

Corresponding author e-mail: [yspei@bnu.edu.cn](mailto:yspei@bnu.edu.cn) Telephone: +86 13910155311

**Abstract:** A fixed-bed system was constructed by sludge-based biochar (SB) for research the influence of different contaminations ( $\text{Zn}^{2+}$ ,  $\text{NH}_4^+$ ,  $\text{H}_2\text{PO}_4^-$ ) on  $\text{Pb}^{2+}$  adsorption in continuous flow. The results reflected that dynamic adsorption capacity ( $q_d$ ) was increased with increasing pH. Under binary-components systems, the inhibition effect of three categories contaminates on  $\text{Pb}^{2+}$  adsorption follow the order as  $\text{NH}_4^+ > \text{Zn}^{2+} > \text{H}_2\text{PO}_4^-$ . When  $\text{H}_2\text{PO}_4^-$  ion exist in ternary or quaternary components system, it depressed the inhibition effect of component systems on  $\text{Pb}^{2+}$  adsorption. Meanwhile, the systems containing  $\text{Zn}^{2+}$  ion showed more significantly impact on the breakthrough curves among all combinations, and the influence of different compound system (①  $\text{Pb}^{2+}$ - $\text{Zn}^{2+}$ - $\text{NH}_4^+$ , ②  $\text{Pb}^{2+}$ - $\text{Zn}^{2+}$ - $\text{H}_2\text{PO}_4^-$ , ③  $\text{Pb}^{2+}$ - $\text{NH}_4^+$ - $\text{H}_2\text{PO}_4^-$ , ④  $\text{Pb}^{2+}$ - $\text{Zn}^{2+}$ - $\text{NH}_4^+$ - $\text{H}_2\text{PO}_4^-$ ) on parameters of breakthrough curves followed the order as ④>②>①>③. In-depth analysis on the change of  $q_d$  and the height of mass transfer zone ( $H$ ) indicated that complicate contaminations system lead to fixed-bed adsorption performance degradation. Additionally, in compared with Yoon-Nelson model, Thomas model can be better used to described the  $\text{Pb}^{2+}$  adsorption process in fixed-bed system, whereas, the application result was drastically affected by co-existing contaminations. The application of model was severely restricted by the complex environmental pollutants, and the interaction effect between adsorbates hindered the prediction performance of model for fixed-bed.

**Keywords:** fixed-bed;  $\text{Pb}^{2+}$ ;  $\text{Zn}^{2+}$ ;  $\text{NH}_4^+$ ;  $\text{H}_2\text{PO}_4^-$ ; combined pollution; continuous flow

## Highlights:

Dynamic adsorption preference of biochar was studied by continuous flow fixed-bed system.

Effect of  $\text{NH}_4^+$ ,  $\text{Zn}^{2+}$ , and  $\text{H}_2\text{PO}_4^-$  on  $\text{Pb}^{2+}$  adsorption were observed in a multi-solute system.

Interaction of contaminants under some condition is conducive to enhance treatment effective.

Thomas and Yoon-Nelson model were applied to describe the adsorption process of  $\text{Pb}^{2+}$  in complex conditions.

## 1.Introduction

In recent years the metallic lead, lead alloys and lead compounds had been widely applied in storage battery, machine building, shipbuilding, light manufacturing, radiation protection, etc[1-4]. However, natural water body have been heavily contaminated by lead wastes in lead application process. Consequently, the treatment and disposal for lead pollution have been the focal and heated point in the field of water environment protection[5-7]. Fixed bed reactor is a key and common technique in waste water treatment fields. The purification capacity of this method is mainly depend on the adsorption capacity of packed adsorbent in column, therefore, the adsorption preference of adsorbate directly impacts the overall purification ability of fixed-bed system.

These several years, the production of activated sludge was increased with the increasing of population and water consumption in urbanization proceeding. Previous investigations have shown that the activated sludge can be used as crude material for adsorption of pollutants through carbonization, their researches proved that the biochar possesses

highly porous structure, special surface chemical behaviors, high thermal stability and wide applied pH range[8-10]. In addition, the biochar can efficiently remove different heavy metals from aqueous solutions [11, 12]. These results indicated that the carbonization process was conducive to enhancing adsorption preference of materials. In view of aforementioned material characteristics, sludge-based biochar has a great potential to be utilized as absorbent in fixed-bed system to eliminate heavy metals from aqueous solution.

Most of published reports about adsorbents focused on surface characteristics of materials and its adsorption capacity for a certain pollution. But, in practice, decontamination process of target pollutants was always influenced by environmental factors and coexisting pollutants [13-15]. In this case, further study and test in complex contamination systems is not only helps to better understanding of the actual adsorption behavior in natural environment, but also confirms the actual removal effect in complex system. Therefore, in order to optimize application environment and reduce the decontamination costs, the further research on complex pollution adsorption in fixed-bed is necessary and inevitable.

Recent studies have reported that lead and zinc element were always coexisted in associated minerals (e.g. sphalerite and galena) [16-18]. Thus, in the smelting, processing and treatment procedure of ore, the combined action of lead and zinc is prerequisite to be taken into account. Meanwhile, the mining is always located in the remote region in general near to agriculture area. In this background, the local natural water body is readily influenced by the mining, processing and transportation procedure of heavy metal. Additionally, based on the requirement of agricultural production, nitrogen fertilizer (major constituent:  $\text{NH}_4\text{NO}_3$ ,  $\text{CO}(\text{NH}_2)_2$ ,  $\text{NH}_4\text{HCO}_3$ , etc.) and phosphate fertilizer (major constituent:  $\text{Ca}(\text{H}_2\text{PO}_4)_2$ ,  $\text{Ca}_3(\text{PO}_4)_2$ ,  $\text{CaSO}_4$ , etc.) were widely applied to the fields[10, 19]. But a majority of fertilizer were not fully utilized and finally leached to local natural water, which led to serious water pollution. In consideration of all aforementioned situation, in order to ascertain the actual treatment efficiency of target contaminant, and clarify the interrelationship between different contaminants, it is necessary to research the actual removal effect of  $\text{Pb}^{2+}$  under the complex environment containing zinc, ammonia and phosphorus.

To date, the study about interaction effect of complex contaminants was focused on the static batch experiment[20-22]. This method can be used to confirm the influence of different pollution on adsorbent under the effect of complex environment in static regime, but it has little reference to the adsorption behavior in dynamic continuous regime. Furthermore, the current studies on interaction effect are still restricted by the research method and analyzing measure, which made it is difficult to elucidate the interaction effect and quantitative relationship between contaminants and removal effect. In this case, the study about influence of complex contaminants on fixed-bed system compensates for the shortcoming of former research. This study both identifies the interaction effect of different contaminants, and solves the problem about quantitative measure of adsorbent capacity under actual environment. It possesses current significance for fixed-bed application at present stage.

In this study, fixed-bed system was constructed by glass columns packed with SSB. The effect of  $\text{Zn}^{2+}$ ,  $\text{NH}_4^+$ ,  $\text{H}_2\text{PO}_4^-$  and their combined systems on fixed-bed adsorption preference for  $\text{Pb}^{2+}$  ion were studied. The effort of different contaminants on breakthrough curves and parameters were calculated and analyzed. The main objective of this study was to determine the adsorption behaviors of  $\text{Pb}^{2+}$  in fixed-bed under complex environment and to clarify the effect mechanisms of different contaminants in detail.

## 2. Materials and methods

### 2.1 Materials

Activated sludge were collected from wastewater treatment plant (Changsha, Hunan, China). The collected sludge were washed to remove dirt and dried in an oven at 105 °C for 24 h. Dried sludge were packed in crucible and placed in a muffle furnace, and then the pyrolysis heating rate was set at 15 °C/min. Then, the sludge were annealed under anaerobic environment at 500 °C for 4 h. Afterwards, all sludge-based biochar (SBB) were sealed and kept in dryer.

### 2.2. Reagents

Lead(II) nitrate [Pb(NO<sub>3</sub>)<sub>2</sub>], zinc(II) nitrate [Zn(NO<sub>3</sub>)<sub>2</sub>·6H<sub>2</sub>O], ammonium nitrate [NH<sub>4</sub>NO<sub>3</sub>], calcium superphosphate [Ca(H<sub>2</sub>PO<sub>4</sub>)<sub>2</sub>] were purchased from Xi Long chemical Co.Ltd (Shantou, Guangdong, China). Analytical grade chemicals were used as received.

### 2.3 Continuous flow fixed-bed adsorption experiments

The fixed-bed experiments were performed by a glass column (internal diameter =10.0 mm, length=250 mm) packed with sludge-based biochar (3.0 g, equiv. to 55 mm of bed depth). Glass wool (10 mm) were packed at the bottom and top of adsorbent to ensure adsorbent fixing and liquid distribution uniformity. The effluents were pumped into column from top to bottom, and the flow rate was maintained at 3.0 mL/min by peristaltic pump. A stock solution of Pb<sup>2+</sup>, Zn<sup>2+</sup>, NH<sub>4</sub><sup>+</sup> and H<sub>2</sub>PO<sub>4</sub><sup>-</sup> were obtained by dissolving the exact quantity of [Pb(NO<sub>3</sub>)<sub>2</sub>], [Zn(NO<sub>3</sub>)<sub>2</sub>·6H<sub>2</sub>O], [NH<sub>4</sub>NO<sub>3</sub>] and [Ca(H<sub>2</sub>PO<sub>4</sub>)<sub>2</sub>] in ultrapure water.

The test solutions containing Pb<sup>2+</sup> ion were prepared by diluting 10.0 mmol/L of stock solutions of metal ions to the 1.0 mmol/L. In effect of pH experiments, the pH of test solutions were adjusted to 3.0, 4.5 and 6.0 by 0.1 M HNO<sub>3</sub> and NaOH. In effect of binary contaminants experiments, the binary solutes solutions of Pb<sup>2+</sup>-Zn<sup>2+</sup>, Pb<sup>2+</sup>-NH<sub>4</sub><sup>+</sup> and Pb<sup>2+</sup>-H<sub>2</sub>PO<sub>4</sub><sup>-</sup> were obtained by diluting and mixing stock solutions of Pb<sup>2+</sup>, Zn<sup>2+</sup>, NH<sub>4</sub><sup>+</sup>, and H<sub>2</sub>PO<sub>4</sub><sup>-</sup> in desired test solutions. And in order to investigated the effect of coexisting contaminants on adsorption of Pb<sup>2+</sup>, the concentration of Pb<sup>2+</sup> (1.0 mmol/L) was remain unchanged and the other three ions were adjusted to 0.5 and 1.0 mmol/L, respectively. In effect of multiple contaminants experiments, the ternary and quarternary solutes solutions of Pb<sup>2+</sup>-Zn<sup>2+</sup>-NH<sub>4</sub><sup>+</sup>, Pb<sup>2+</sup>-Zn<sup>2+</sup>-H<sub>2</sub>PO<sub>4</sub><sup>-</sup>, Pb<sup>2+</sup>-NH<sub>4</sub><sup>+</sup>-H<sub>2</sub>PO<sub>4</sub><sup>-</sup> and Pb<sup>2+</sup>-Zn<sup>2+</sup>-NH<sub>4</sub><sup>+</sup>-H<sub>2</sub>PO<sub>4</sub><sup>-</sup> were obtained by diluting and mixing stock solutions in test solutions, and all solutes were keep in same concentration (1.0 mmol/L).

And then, the solutions with different pH and contaminants were pumped into fixed-bed, and the effluents were collected at regular time intervals (10 min) and the concentration of Pb<sup>2+</sup> was measured by Flame Atomic Absorption Spectrometry (AAS3500, Thermo Electron Corporation, USA).

### 2.4 Calculation of breakthrough parameters of fixed-bed

The breakthrough curve reflects the adsorption performance of fixed-bed. The parameters of fixed-bed are important characteristics for determining the operation and dynamic response of adsorbent that packed in column [23, 24]. In this study, the total mass of Pb<sup>2+</sup> ion adsorbed by fixed-bed ( $M_{ad}$ , mmol) and the dynamic adsorption capacity ( $q_d$ , mmol/L) can be calculated as the following (Eq. (1) and Eq. (2)):

$$M_{ad} = \frac{Q}{1000} \int_0^{t_e} (C_0 - C_t) dt \quad (1)$$

$$q_d = \frac{M_{ad}}{m} \quad (2)$$

where  $Q$  is the rate of flow (mL/min),  $C_0$  and  $C_t$  are the  $Pb^{2+}$  ions' concentration (mmol/L) of before and after treatment, respectively,  $t_b$  and  $t_e$  are the time (min) of breakthrough point ( $C_t/C_0=10\%$ ) and saturation point ( $C_t/C_0=95\%$ ), respectively,  $m$  is the mass of the SBB packed in column (g).

The height of mass transfer zone ( $H$ ) indicated the utilization efficiency of adsorbent in column, this parameter can be calculated from equation(3):

$$H = \frac{C_0 Q (t_e - t_b)}{1000 \rho q_d A} \quad (3)$$

where  $\rho$  is the packed density ( $g/cm^3$ ) of SSB,  $A$  is the cross-sectional area of column.

Additionally, the total mass of metal through fixed-bed system ( $M_{total}$ , mmol) and the total metal removal rate of fixed-bed ( $R$ , %) can be calculated from the following equation (4) and (5), respectively.

$$M_{total} = \frac{C_0 Q t_{total}}{1000} \quad (4)$$

$$R = \frac{M_{ad}}{M_{total}} \quad (5)$$

### 3. Results and Discussion

#### 3.1 Breakthrough curve of $Pb^{2+}$ ion adsorption process under different pH

As presented in Figure 1, the breakthrough curves of  $Pb^{2+}$  adsorption process under pH=4.5 and pH=6.0 were intersected with the other, this result indicated that the adsorption performance of SBB fixed-bed was little change when pH down from 6.0 to 4.5. However, compared with that at pH 6.0, the breakthrough curve of  $Pb^{2+}$  was significantly shifted to left under pH 3.0. Meanwhile, the slope of curve was clearly increased with decreasing pH. These phenomenon were mainly due to the influence of  $H^+$  ion on adsorbent. In compared with  $Pb^{2+}$  concentration (1.00 mmol/L), the  $H^+$  ion concentration was relatively lower in pH range of 4.5-6.0, which only showed a limited impact on  $Pb^{2+}$  adsorption. But at pH 3.0,  $H^+$  ion concentration (1.00 mmol/L) was high enough to influence adsorption behavior of  $Pb^{2+}$ . Mass research results[1, 25, 26] have demonstrated that the high concentrations of  $H^+$  ion significantly affect  $Pb^{2+}$  adsorption through material surface protonation effect and active sites competition effect, and these effects were increased with decreasing pH just like the results in this study. In view of the adsorption performance of system is strongly influenced by  $H^+$  ion, the pH should be considered as a key design parameters in the application of fixed-bed.

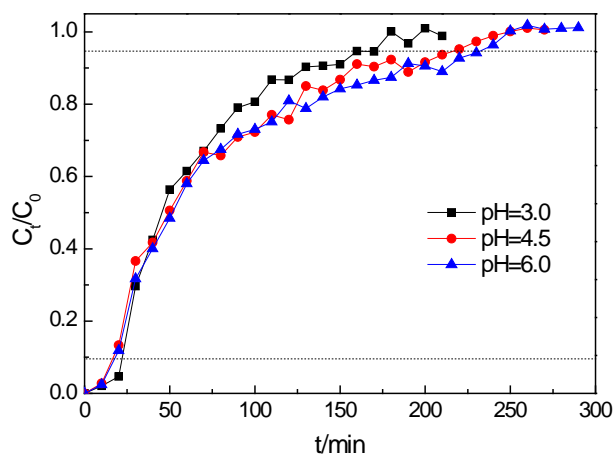


Figure 1 The breakthrough curves of  $Pb^{2+}$  ion in fixed-bed adsorption system under impact of pH.

The parameters of Table 1 were calculated by the data of breakthrough curves in Figure 1. From the results in Table 1, it was clear that the breakthrough time ( $t_b$ ) of different pH were reached in a short time (within 23 min). Comparing to the change of exhaustion time ( $t_e$ ) with variation of pH, the  $t_b$  was hardly changed by pH, and it almost all happened within the second interval test. A reasonable explanation for these results maybe due to the  $H^+$  ion was neutralized by alkaline biochar at an early stage. And then, with continuous input of solutions, the  $H^+$  ions' effect on adsorbent was increased along with  $t$ , and resulted in the system exhaustion emerged in shorter time. The dynamic adsorption capacity ( $q_d$ ) for pH of 3.0, 4.5 and 6.0 were 0.0553, 0.0638 and 0.0732 mmol/g, respectively. This tendency clearly indicated that the SBB adsorption capacity was inhibited at relatively low pH. It is worth noting here that the height of mass transfer zone ( $H$ ) was decreased with increasing  $H^+$  ion concentration, which meant that the utilization rate of fixed-bed system was increased. This phenomenon can be attributed to that the major non-specific adsorption sites were occupied by  $H^+$  ion at lower pH, and then, the remanent specific sites possess stronger affinity and they can adsorb  $Pb^{2+}$  through weaker mass transfer force, which caused the irrational change of  $H$ . In subsequent research, the curve in pH of 4.5 was chosen as reference under the consideration of most multi-components solutions were in the pH around 4.5.

Table 1 The breakthrough curve parameters of  $Pb^{2+}$  under impact of pH

pH	$t_b$ /(min)	$t_e$ /(min)	$M_{ad}$ /(mmol)	$M_{total}$ /(mmol)	$q_d$ /(mmol/g)	$H$ /(cm)	$R$ /%
3.0	22.13	169.99	0.1659	0.4309	0.0553	27.11	38.51
4.5	18.30	217.13	0.1915	0.5504	0.0638	31.59	34.79
6.0	16.92	232.37	0.2195	0.5891	0.0732	29.86	37.26

### 3.2 Breakthrough curve of $Pb^{2+}$ ion adsorption process under different contaminants

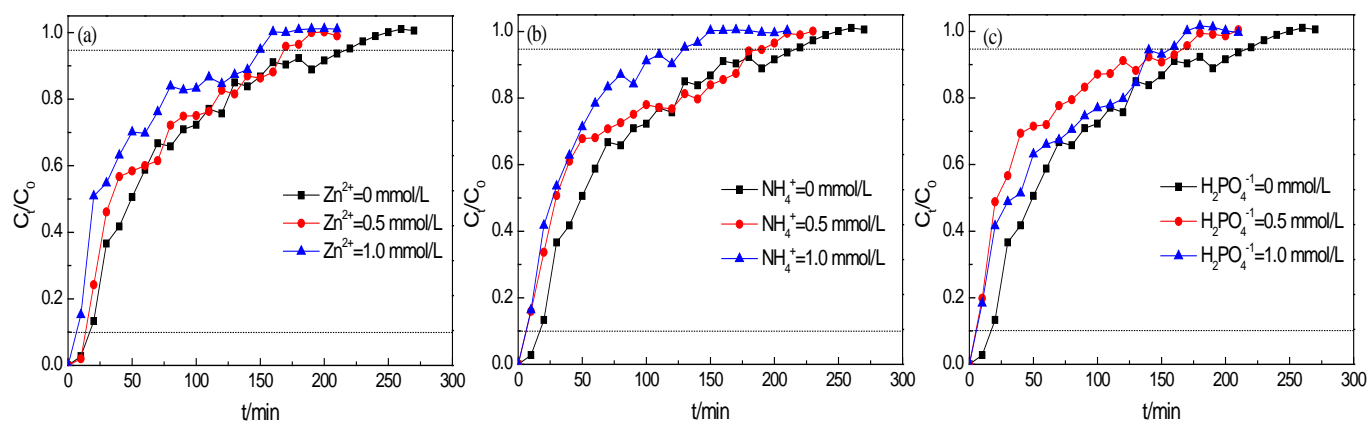


Figure 2 The breakthrough curves of  $Pb^{2+}$  ion in fixed-bed system under impact of  $Zn^{2+}$ ,  $NH_4^+$ , and  $H_2PO_4^-$

In order to reduce the impact of anion on experiment, the cation contaminants solutions were made of lead nitrate [ $Pb(NO_3)_2$ ], zinc nitrate [ $Zn(NO_3)_2 \cdot 6H_2O$ ] and ammonium nitrate [ $NH_4NO_3$ ], respectively. Furthermore, thus far, there were many investigators had researched the adsorption preference of calcium alginate and calcium-modified materials for heavy metal[27-29]. Thus, it can be inferred from their results that the  $Pb^{2+}$  adsorption was insignificantly affected by the existence of  $Ca^{2+}$  ion in aqueous solution. Based on this, the superphosphate [ $Ca(H_2PO_4)_2$ ] was used to research the anion effect on  $Pb^{2+}$  ion adsorption. For investigate the different contaminations effect on breakthrough curves of  $Pb^{2+}$

adsorption in fixed-bed system, the combined contaminations solutions were synthesized by aforementioned reagents, and the results were presented in Figure 2.

Figure 2a depicts the influence of  $Zn^{2+}$  on  $Pb^{2+}$  ion, the profiles of curve indicated that the SSB adsorption performance for  $Pb^{2+}$  was inhibited by  $Zn^{2+}$  ion. Moreover, the inhibition become greater as the concentration increased. Generally, coexisting ions in solutions will compete for active sites in liquid-solid adsorption system, which degrade the adsorption capacity for mono ion [30, 31]. By contrast, in this study the fixed-bed exhausted its adsorption effect in shorter time when  $Zn^{2+}$  ion exist in solutions. Furthermore, higher concentration of  $Zn^{2+}$  ion increased its mass transfer driving force, and enhanced the competitive effect of  $Zn^{2+}$  ion. So the breakthrough curve of  $Pb^{2+}$  was affected by  $Zn^{2+}$  ion more significant in higher  $Zn^{2+}$  ion concentration ( $c(Zn^{2+})=1.0$  mmol/L).

Similarly,  $NH_4^+$  ion shows inhibition effect on  $Pb^{2+}$  ions' breakthrough curves just like  $Zn^{2+}$  ion (Figure 2b). However, the change of breakthrough curve was different to the effect of  $Zn^{2+}$ . The change under influence of  $Zn^{2+}$  was relatively steady during the whole process. But under the effect of  $NH_4^+$  ion ( $c(NH_4^+)=0.5$  mmol/L), there was significant change in the slope of curve at  $t=60$  min. Since then, the slope of  $Pb^{2+}$ - $NH_4^+$  system was nearly parallel to that of single ion system. Which is in fact maybe attributed to the abundant adsorption sites in the early stage, when the  $Pb^{2+}$  and  $NH_4^+$  can be effective adsorbed, but with continuous input of  $Pb^{2+}$  ( $c(Pb^{2+})=1.0$  mmol/L), the  $NH_4^+$  was easily displaced by  $Pb^{2+}$  and caused the slope of breakthrough curve was close to that of single ion system. In contrast, the curve of higher  $NH_4^+$  concentration was not analogous to above-mentioned facts, it is ascribed that the release resistance was strong enough to impede the displacement when  $c(NH_4^+)=1.0$  mmol/L.

The breakthrough curves of  $Pb^{2+}$  under the effect of  $H_2PO_4^-$  ion are presented in Figure 2c. The change of breakthrough curves by  $H_2PO_4^-$  was more significant than that of  $Zn^{2+}$  and  $NH_4^+$  when  $c(H_2PO_4^-)=0.5$  mmol/L. But there were a obvious right shift in breakthrough curves when  $H_2PO_4^-$  ion concentration increased from 0.5 to 1.0 mmol/L, this phenomenon showed a reverse trend to that in  $Zn^{2+}$  or  $NH_4^+$  effect. Based on the above results, the mechanism of  $H_2PO_4^-$  effect on  $Pb^{2+}$  adsorption could be divided into two aspects: ①at a lower concentration,  $H_2PO_4^-$  and  $Pb^{2+}$  were competed for adsorption sites where can adsorb  $H_2PO_4^-$  and  $Pb^{2+}$  simultaneously, which inhibited the adsorption of  $Pb^{2+}$ ; ②at a higher concentration, excess  $H_2PO_4^-$  ion reacted with the cation (neutralize the positive charge) that excessive accumulated on the adsorbent, which reduced the electrostatic potential at the adsorbent surface, and in this case, the reaction decreased the repulsive force between surface field and cation, and then facilitated  $Pb^{2+}$  ion adsorption. This induction effect of phosphate on cation was also observed in the research of Talebi Atouei et al [32]. However, due to a certain quantity of shared sites were occupied by  $H_2PO_4^-$  ion, compared with the single ion system, the adsorption capacity of biochar for  $Pb^{2+}$  was still inhibited to some extent.

### 3.3 Breakthrough curve of $Pb^{2+}$ adsorption process under multiple contaminants

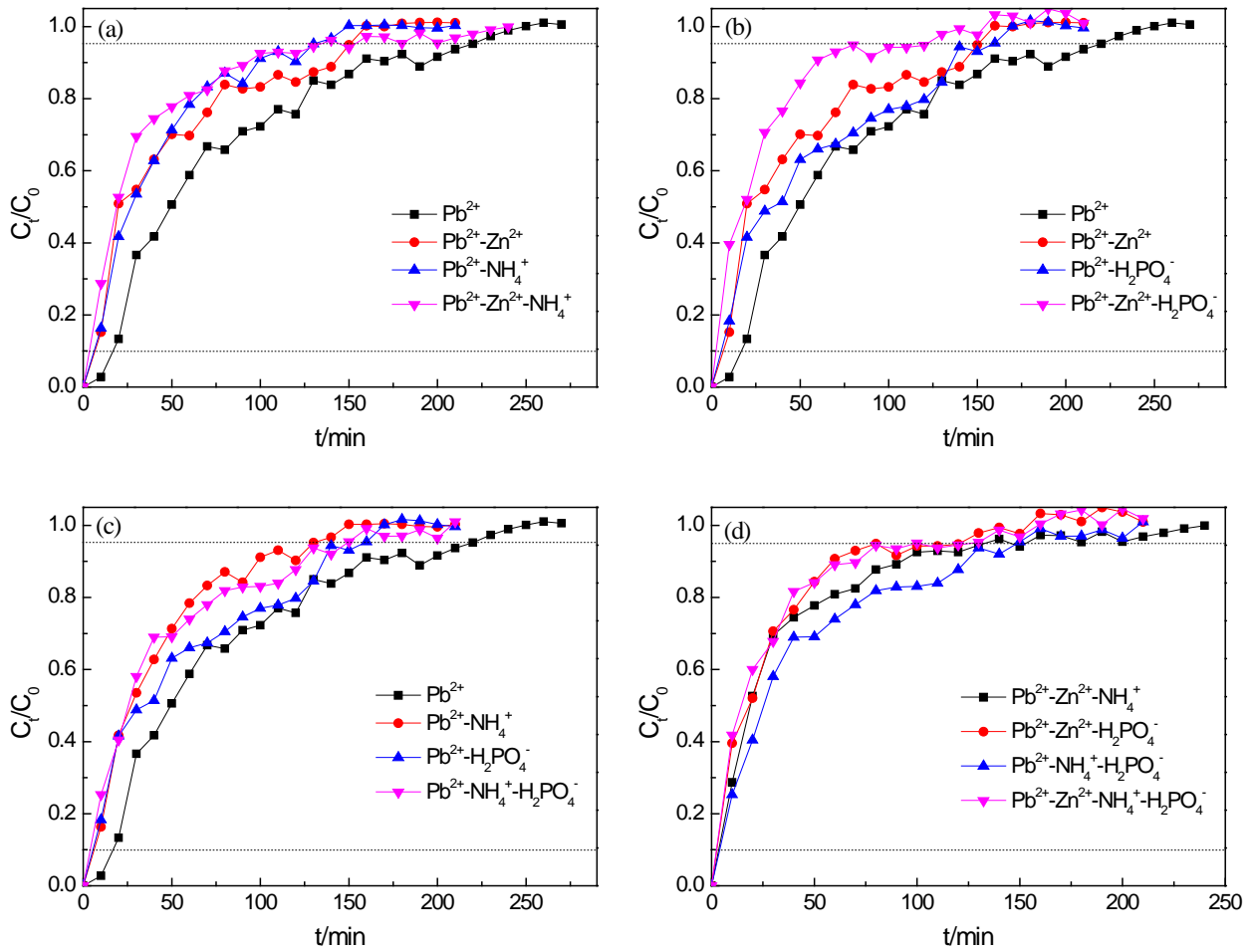


Figure 3 The breakthrough curves of  $\text{Pb}^{2+}$  in fixed-bed adsorption system under complex conditions

Figure 3 shows the breakthrough curves of  $\text{Pb}^{2+}$  under the effect of multiple contaminations systems. As presented in Figure 3a, the influence of  $\text{NH}_4^+$  on breakthrough curve was more significant than that of  $\text{Zn}^{2+}$  at coexisting ions concentration of 1.0 mmol/L. By comparing the results in Figure 3a and 3b, the influence of three contaminations on the  $\text{Pb}^{2+}$  ion adsorption were in the order of  $\text{NH}_4^+ > \text{Zn}^{2+} > \text{H}_2\text{PO}_4^-$ . Additionally, in the  $\text{Pb}^{2+}$ - $\text{Zn}^{2+}$ - $\text{H}_2\text{PO}_4^-$  ternary-solute system, there were no sign of the aforementioned facilitated effect of  $\text{H}_2\text{PO}_4^-$ , this result maybe due to the existence of excess  $\text{Zn}^{2+}$  ion (bivalent) provided abundant positive charge to neutralize negative charge. Therefore, the facilitated effect of  $\text{H}_2\text{PO}_4^-$  was counteracted by  $\text{Zn}^{2+}$  in ternary-solute system.

As shown in Figure 3c,  $\text{Pb}^{2+}$ - $\text{NH}_4^+$ - $\text{H}_2\text{PO}_4^-$  ternary-solute system indicated less influence on breakthrough curves than  $\text{Pb}^{2+}$ - $\text{NH}_4^+$  binary-solute system. It can be inferred that the addition of  $\text{H}_2\text{PO}_4^-$  would neutralize the positive charge on the material surface (or the liquid film which near to the solid phase) and thus reduce the repulsive forces, leading to the inhibition effect of  $\text{NH}_4^+$  was counteracted. Consequently, the adsorption performance of fixed-bed in this ternary-solute system was better than binary-solute system. This phenomenon indicated that the interaction of different contaminations under some condition was conducive to enhancing effective of fixed-bed, further research on this mechanism was important to the development of multiple contaminants simultaneous treatment technology.

In Figure 3d, the influence of different compound system (① $\text{Pb}^{2+}$ - $\text{Zn}^{2+}$ - $\text{NH}_4^+$ , ② $\text{Pb}^{2+}$ - $\text{Zn}^{2+}$ - $\text{H}_2\text{PO}_4^-$ , ③ $\text{Pb}^{2+}$ - $\text{NH}_4^+$ - $\text{H}_2\text{PO}_4^-$ , ④ $\text{Pb}^{2+}$ - $\text{Zn}^{2+}$ - $\text{NH}_4^+$ - $\text{H}_2\text{PO}_4^-$ ) on breakthrough curve followed the order as ④>②>①>③. In -depth

analysis on this order revealed that the existence of  $\text{H}_2\text{PO}_4^-$  reduced the impact of coexisting contaminations on the  $\text{Pb}^{2+}$  adsorption in fixed-bed. On the contrary, the multiple systems containing  $\text{Zn}^{2+}$  showed more inhibition effect on the breakthrough curves than others. The observed phenomenon in this study implied that rational simultaneous dispose of different categories may helpful to promote effective in treatment technology.

### 3.4 The parameters of breakthrough curves

For further analysis on numerical relationship between contaminations and fixed-bed systems, the parameters and variation were calculated and summarized in the Table 2. The  $t_b$  and  $t_e$  value presented in Table 2 demonstrated that the breakthrough and exhaustion time of all multiple systems were reached in shorter time compared to single ion solution. The variation (i.e.  $\Delta t_b$  and  $\Delta t_e$ ) were all negative, which meant that the coexisting contaminations cancelled out the adsorption effects of fixed-bed, and made adsorbate breakthrough in less time. Beside the  $\text{Pb}^{2+}\text{-H}_2\text{PO}_4^-$  and  $\text{Pb}^{2+}\text{-NH}_4^+\text{-H}_2\text{PO}_4^-$  systems, the higher concentration and the more contaminations in the solutions, the shorter time the fixed-bed reached its saturation point, and those variation were consistent with the change of breakthrough profiles in Figure 2 and 3. The  $M_{ad}$  and  $M_{total}$  were mainly calculated by the surface integral of breakthrough curves and  $t_e$ , respectively. As presented in Table 2, the  $\Delta M_{ad}$  were all negative, and the changing trend of the  $M_{ad}$  and  $t_e$  were accordant with each other. But, in view of the great changes of the shape and parameters of breakthrough curves, the variation of  $M_{ad}$  and  $M_{total}$  in different systems were unpredictable. Therefore, these two parameters have little significance in adsorption comparison study. Meanwhile, the removal rate ( $R$ ) was ratio of  $M_{ad}$  to  $M_{total}$ , but  $\Delta R$  was also irregular with the change of different systems. These data indicated that  $M_{ad}$ ,  $M_{total}$  and  $R$  were not applicable for direct estimation the fixed-bed adsorption performance in complex environment.

Table 2 The breakthrough curve parameters and variations of  $\text{Pb}^{2+}$  under impact of  $\text{Zn}^{2+}$ ,  $\text{NH}_4^+$ , and  $\text{H}_2\text{PO}_4^-$

System	co-existence ions concentration/ mmol/L	$t_b$ /	$t_e$ /	$M_{ad}$ /	$M_{total}$ /	$R$ /	$\Delta t_b$ /	$\Delta t_e$ /	$\Delta M_{ad}$ /	$\Delta M_{total}$ /	$\Delta R$ /
		min	min	mmol	mmol	%	min	min	mmol	mmol	%
$\text{Pb}^{2+}$	-	18.30	217.13	0.1915	0.5504	34.79	-	-	-	-	-
$\text{Pb}^{2+}\text{-Zn}^{2+}$	0.5	13.98	169.12	0.1855	0.4287	42.07	-4.32	-48.01	-0.0060	-0.1217	7.28
	1.0	6.90	150.06	0.1546	0.3804	39.52	-11.40	-67.07	-0.0369	-0.1700	4.73
$\text{Pb}^{2+}\text{-NH}_4^+$	0.5	6.33	192.56	0.1893	0.5297	35.73	-11.97	-24.57	-0.0022	-0.0207	0.94
	1.0	6.08	129.82	0.1582	0.3571	44.29	-12.22	-87.31	-0.0333	-0.1933	9.50
$\text{Pb}^{2+}\text{-H}_2\text{PO}_4^-$	0.5	5.64	158.27	0.1024	0.4354	23.51	-12.66	-58.86	-0.0891	-0.1150	-11.28
	1.0	5.13	167.43	0.1405	0.4606	30.50	-13.17	-49.70	-0.0510	-0.0898	-4.29
$\text{Pb}^{2+}\text{-Zn}^{2+}$ $\text{-NH}_4^+$	1.0/1.0	3.34	132.34	0.0778	0.3641	21.37	-14.96	-84.79	-0.1137	-0.1864	-13.42
$\text{Pb}^{2+}\text{-Zn}^{2+}$ $\text{-H}_2\text{PO}_4^-$	1.0/1.0	2.85	121.55	0.0364	0.3344	10.88	-15.45	-95.58	-0.1551	-0.2160	-23.91
$\text{Pb}^{2+}\text{-NH}_4^+$ $\text{-H}_2\text{PO}_4^-$	1.0/1.0	4.07	148.98	0.1087	0.4098	26.53	-14.23	-68.15	-0.0828	-0.1406	-8.26
$\text{Pb}^{2+}\text{-Zn}^{2+}$ $\text{-NH}_4^+\text{-H}_2\text{PO}_4^-$	1.0/1.0/1.0	2.40	126.93	0.0626	0.3492	17.92	-15.90	-90.20	-0.1289	-0.2012	-16.87

Dynamic adsorption capacity ( $q_d$ ) and the height of mass transfer zone ( $H$ ) were calculated by Eq. (2) and Eq. (3), respectively. These two parameters represent the adsorption performance of unit mass and unit volume, respectively, and they can be used to describe the adsorption capacity of fixed-bed. Contrast study of  $q_d$  and  $H$  under the effect of different factors is help to better understand the quantitative influence of contaminations on fixed-bed system. It can be seen from Figure 4 that compared to single ion system, the  $q_d$  under effect of different contaminations presented significantly decreased except the  $Pb^{2+}$ - $NH_4^+$  system when  $c(NH_4^+)=0.5$  mmol/L(the reason for this phenomenon have been analyzed in section 3.2). The value change of  $q_d$  revealed that the adsorption capacity for  $Pb^{2+}$  of SBB was strongly inhibited by coexisting ions in system. The highest  $q_d$  (0.0638 mmol/g) was observed in single ion system and the lowest  $q_d$  (0.0121 mmol/g) was under the effect of  $Pb^{2+}$ - $Zn^{2+}$ - $H_2PO_4^-$  compound system. These results demonstrated that multiple components showed a complex interaction in the adsorption process and strong influence on the treatment efficiency. Therefore, the treatment of coexisting contaminations is an inevitable important issue in design and application of fixed-bed system.

The height of ( $H$ ) represents the actual length of adsorbent column which play their adsorption role in the process of fixed-bed operation. Generally, the shorter  $H$  means that the higher utilization efficiency. On the contrary, the longer  $H$  implies that the fixed-bed need the thicker bed to adsorb contaminations [33]. By comparing the Figure 4 and 5, the results indicated that the variation of  $H$  showed opposite tendency to that of  $q_d$  in the corresponding systems, and the fixed-bed need more adsorbent to adsorb unit mass  $Pb^{2+}$  ion in the effect of multiple contaminations. But under the  $Pb^{2+}$ - $NH_4^+$ - $H_2PO_4^-$  system, compared to the other ternary-solute and quaternary-solute solutions, the  $H$  and  $q_d$  showed distinct advantage. In this situation, the inhibition effect on SBB was minimal. This result demonstrated that the simultaneous treatment of  $Pb^{2+}$ ,  $NH_4^+$ , and  $H_2PO_4^-$  in fixed-bed system maybe a viable method.

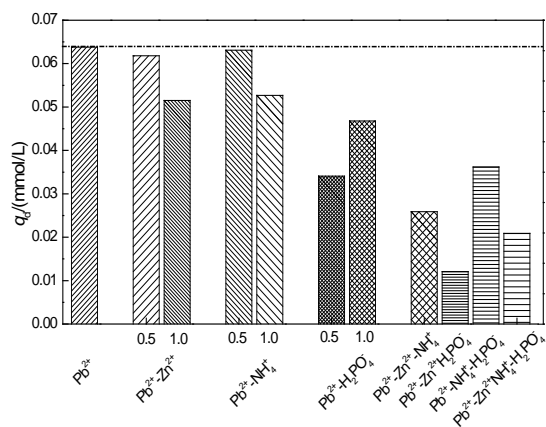


Figure 4 The dynamic adsorption capacity ( $q_d$ ) of fixed-bed in different systems

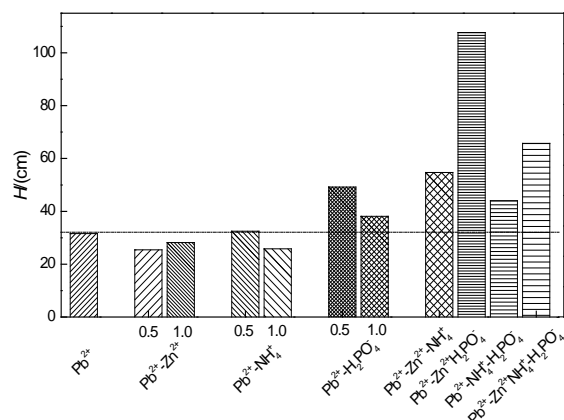


Figure 5 The height of transfer zone ( $H$ ) of fixed-bed in different systems

### 3.5 Thomas model and Yoon-Nelson model

The Thomas model and Yoon-Nelson model were used for the in-depth analysis of breakthrough curves. The linear form of two models were respectively given by equation (11) and (12):

$$\ln\left(\frac{C_t}{C_0} - 1\right) = K_{Th} q_{md} \frac{m}{Q} - K_{Th} C_0 t \quad (11)$$

$$\ln\left(\frac{C_t}{C_0 - C_t} - 1\right) = K_{YN} t - \tau K_{YN} \quad (12)$$

where  $K_{Th}$  and  $K_{YN}$  are the Thomas model rate constant [ $10^{-3}L/(min \cdot mmol)$ ] and Yoon-Nelson model rate constant (L/min), respectively,  $q_{md}$  is the maximum dynamic adsorption capacity (mmol/g),  $\tau$  is the time required for 50% adsorbate breakthrough (min). The results of data fitting and model parameters were demonstrated in Figure 7 and Table 4, respectively.

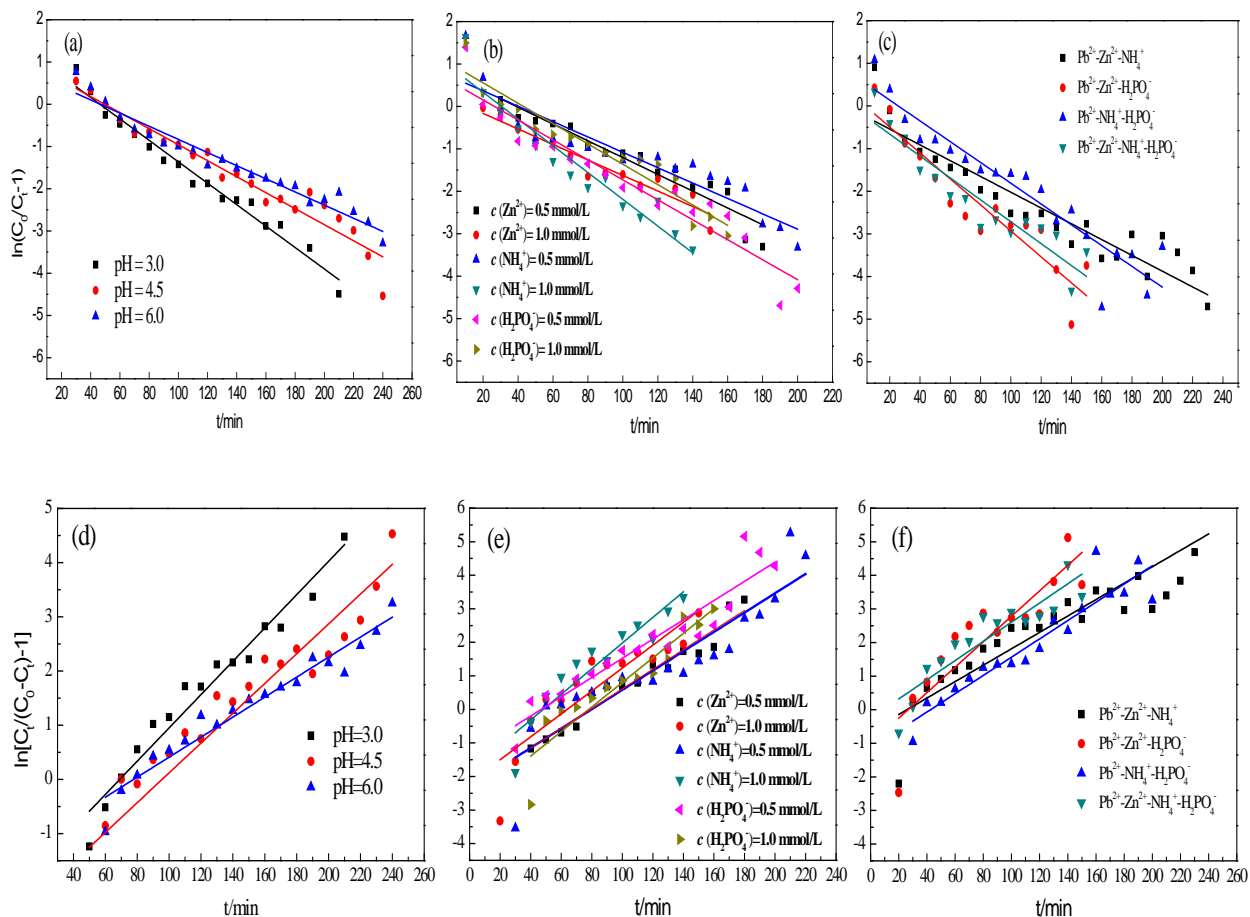


Figure 6 The fitting curves of Thomas model(a, b, c) and Yoon-Nelson model (d, e, f) for breakthrough curves of  $Pb^{2+}$  ion in different systems

The data of  $Pb^{2+}$  adsorption breakthrough curves were fitted by Thomas model and Yoon-Nelson model (Figure 6), and model parameters were summarized in Table 3. Dong and Lin[23] and Soto et al [34] have researched the use of Thomas model in the fixed-bed, their studies have confirmed that this model can be used to describe the adsorption with neither interaction between the adsorbed molecules nor axial dispersion in adsorption process. It can be seen from Figure 6 and Table 3 that the fitting curves and results ( $R^2=0.9704\sim 0.9788$ ) were consistent well with the observation data under the single  $Pb^{2+}$  system. Then, as showed in Table 3, under the effect of binary-contaminations, fitting efficiency of Thomas model was clearly decreased ( $R^2=0.8678\sim 0.9253$ ). And the  $NH_4^+$  ion showed strongest influence on  $R^2$  variation among three contaminations. Based on the assumption of Thomas model, this result indicated that the  $NH_4^+$  strongly affects the interaction effect of adsorbed adsorbate and restricts the fitting effect of Thomas model.

The Yoon-Nelson model was based on the assumption that the decrease of adsorption rate for adsorbate is proportional to the probability of adsorbate adsorption, and this model can be used to predict the time of 50% adsorbate

breakthrough the fixed-bed. As seen from Figure 6d, e, f, the data point in fitting curves of Yoon-Nelson model were more disrupt and far away from fitted straight line compared to corresponding lines in Figure 6a, b, c. According to the data in Table 3, the rate constant  $K_{TH}$  and  $K_{YN}$  were close to each other, but the  $R^2$  of Yoon-Nelson model were obviously lower than Thomas model. Moreover, the parameters' variation of Yoon-Nelson model was more strongly affected by complex environment condition than that of Thomas model.

Furthermore, as shown in Table 3, the fitting effect of model was decreased with increasing of contamination category, and the  $R^2$  values of two models, under ternary and quarternary compound systems, were within the range of 0.8729 to 0.8941 and 0.7658 to 0.8867, respectively. Those results manifested that the application of Thomas model and Yoon-Nelson model was severely restricted by the complex environmental pollutants, and the interaction effect between adsorbates hindered the prediction performance of model for fixed-bed. Based on the above results and discussion, it can be concluded that Thomas model can be better used to described the  $Pb^{2+}$  adsorption process in fixed-bed system. Whereas, the application result was drastically affected by coexisting contaminations. Consequently, in order to predict and optimize of fixed-bed operation parameters in natural complex environmental pollutants, it is necessary to further develop a new extension model containing multi-components factors.

Table 3 The parameters of Thomas model and Yoon-Nelson model

System	co-existence ions concentration	Thomas model			Yoon-Nelson model		
		$K_{Th}$	$q_{md}$	$R^2$	$K_{YN}$	$\tau$	$R^2$
$Pb^{2+}$	pH=3.0	0.0301	0.0391	0.9738	0.0314	69.55	0.9396
	pH=4.5	0.0225	0.0522	0.9788	0.0275	95.50	0.8403
	pH=6.0	0.0185	0.0636	0.9704	0.0185	77.55	0.9485
$Pb^{2+}$ - $Zn^{2+}$	0.5	0.0234	0.0330	0.9205	0.0293	74.54	0.9515
	1.0	0.0217	0.0093	0.9253	0.0341	63.98	0.7990
$Pb^{2+}$ - $NH_4^+$	0.5	0.0197	0.0370	0.8678	0.0279	79.32	0.7918
	1.0	0.0344	0.0281	0.9197	0.0341	54.00	0.8767
$Pb^{2+}$ - $H_2PO_4^-$	0.5	0.0256	0.0243	0.9097	0.0287	46.81	0.8925
	1.0	0.0262	0.0396	0.9216	0.0366	78.08	0.8633
$Pb^{2+}$ - $Zn^{2+}$ - $NH_4^+$	1.0/1.0	0.0202	0.0085	0.8813	0.0244	25.75	0.7853
$Pb^{2+}$ - $Zn^{2+}$ - $H_2PO_4^-$	1.0/1.0	0.0333	0.0035	0.8729	0.0379	26.58	0.7658
$Pb^{2+}$ - $NH_4^+$ - $H_2PO_4^-$	1.0/1.0	0.0266	0.0235	0.8941	0.0272	42.55	0.8867
$Pb^{2+}$ - $Zn^{2+}$ - $NH_4^+$ - $H_2PO_4^-$	1.0/1.0/1.0	0.0280	0.0053	0.8750	0.0286	8.72	0.8323

#### 4.conclusion

In this work, a low-cost sludge-based biochar (SSB) was successfully prepared by active sludge and was developed for removal  $Pb^{2+}$  from aqueous solutions. A fixed-bed system was constructed by SSB for research the influence of different contaminations on  $Pb^{2+}$  adsorption in continuous flow. The study of the pH effect suggested that dynamic adsorption capacity  $q_d$  in pH of 6.0, 4.5, and 3.0 were 0.0732, 0.0638, and 0.0553 mmol/g, respectively. Under binary-components systems, the inhibition effect of three categories contaminates on  $Pb^{2+}$  adsorption follow the order as  $NH_4^+ > Zn^{2+} > H_2PO_4^-$ . When  $H_2PO_4^-$  ion exist in ternary or quaternary components system, it depressed the inhibition effect of component systems on  $Pb^{2+}$  adsorption. Meanwhile, the systems containing  $Zn^{2+}$  showed the more significant

impact on the breakthrough curves among all combinations, and the influence of different compound system ( $\text{Pb}^{2+}\text{-Zn}^{2+}\text{-NH}_4^+$ ,  $\text{Pb}^{2+}\text{-Zn}^{2+}\text{-H}_2\text{PO}_4^-$ ,  $\text{Pb}^{2+}\text{-NH}_4^+\text{-H}_2\text{PO}_4^-$ ,  $\text{Pb}^{2+}\text{-Zn}^{2+}\text{-NH}_4^+\text{-H}_2\text{PO}_4^-$ ) on breakthrough curves' parameters followed the order as  $\text{④}>\text{②}>\text{①}>\text{③}$ . In-depth analysis on the variation of  $q_d$  and  $H$  indicated that complicate contaminations system lead to fixed-bed adsorption performance degradation. Furthermore, in compared with Yoon-Nelson model, Thomas model can be better used to described the  $\text{Pb}^{2+}$  adsorption process in fixed-bed system, whereas, the application result was drastically affected by co-existing contaminations. The application of model was severely restricted by the complex contaminants, and the interaction effect between adsorbates hindered the prediction performance of model for fixed-bed.

### Acknowledgement

This work was financially supported by the National Natural Science Foundation of China (Project no. 51579009) and the Major Science and Technology Program for Water Pollution Control and Treatment (Project no. 2018ZX07110005).

### Reference

- [1] N.A. Medellin-Castillo, E. Padilla-Ortega, M.C. Regules-Martínez, R. Leyva-Ramos, R. Ocampo-Pérez, C. Carranza-Alvarez, Single and competitive adsorption of Cd(II) and Pb(II) ions from aqueous solutions onto industrial chili seeds (*Capsicum annuum*) waste, *Sustainable Environment Research*, 27 (2017) 61-69.
- [2] W. Zhang, J. Yang, X. Wu, Y. Hu, W. Yu, J. Wang, J. Dong, M. Li, S. Liang, J. Hu, R.V. Kumar, A critical review on secondary lead recycling technology and its prospect, *Renewable and Sustainable Energy Reviews*, 61 (2016) 108-122.
- [3] H. Cheng, Y. Hu, Lead (Pb) isotopic fingerprinting and its applications in lead pollution studies in China: a review, *Environmental pollution*, 158 (2010) 1134-1146.
- [4] L. Wang, H. Zhang, W. Zhang, G. Cao, H. Zhao, Y. Yang, Enhancing cycle performance of lead-carbon battery anodes by lead-doped porous carbon composite and graphite additives, *Materials Letters*, 206 (2017) 113-116.
- [5] A. Garcia-Alix, F.J. Jimenez-Espejo, J.A. Lozano, G. Jimenez-Moreno, F. Martinez-Ruiz, L. Garcia Sanjuan, G. Aranda Jimenez, E. Garcia Alfonso, G. Ruiz-Puertas, R.S. Anderson, Anthropogenic impact and lead pollution throughout the Holocene in Southern Iberia, *The Science of the total environment*, 449 (2013) 451-460.
- [6] K.M. Burns, J.M. Shoag, S.S. Kahlon, P.J. Parsons, P.E. Bijur, B.H. Taragin, M. Markowitz, Lead Aprons Are a Lead Exposure Hazard, *Journal of the American College of Radiology : JACR*, 14 (2017) 641-647.
- [7] X. Lu, X.A. Ning, P.H. Lee, K. Shih, F. Wang, E.Y. Zeng, Transformation of hazardous lead into lead ferrite ceramics: Crystal structures and their role in lead leaching, *Journal of hazardous materials*, 336 (2017) 139-145.
- [8] S.H. Ho, Y.D. Chen, Z.K. Yang, D. Nagarajan, J.S. Chang, N.Q. Ren, High-efficiency removal of lead from wastewater by biochar derived from anaerobic digestion sludge, *Bioresource technology*, (2017).
- [9] H. Wang, M. Feng, F. Zhou, X. Huang, D.C.W. Tsang, W. Zhang, Effects of atmospheric ageing under different temperatures on surface properties of sludge-derived biochar and metal/metalloid stabilization, *Chemosphere*, 184 (2017) 176-184.
- [10] J. Chen, S. Lu, Z. Zhang, X. Zhao, X. Li, P. Ning, M. Liu, Environmentally friendly fertilizers: A review of materials used and their effects on the environment, *The Science of the total environment*, 613-614 (2017) 829-839.
- [11] J. Iftikhar, J. Wang, Q. Wang, T. Wang, H. Wang, A. Khan, A. Jawad, T. Sun, X. Jiao, Z. Chen, Highly Efficient Lead Distribution by Magnetic Sewage Sludge Biochar: Sorption Mechanisms and Bench Applications, *Bioresource technology*, 238 (2017) 399-406.
- [12] S. Duan, W. Ma, Y. Pan, F. Meng, S. Yu, L. Wu, Synthesis of magnetic biochar from iron sludge for the enhancement of Cr (VI) removal from solution, *Journal of the Taiwan Institute of Chemical Engineers*, (2017).

- [13] X. Liu, D. Yi, Y. Cui, L. Shi, X. Meng, Adsorption desulfurization and weak competitive behavior from 1-hexene over cesium-exchanged Y zeolites (CsY), *Journal of Energy Chemistry*, (2017).
- [14] V. Hernandez-Montoya, M.A. Perez-Cruz, D.I. Mendoza-Castillo, M.R. Moreno-Virgen, A. Bonilla-Petriciolet, Competitive adsorption of dyes and heavy metals on zeolitic structures, *Journal of environmental management*, 116 (2013) 213-221.
- [15] J.J. Gonzalez Costa, M.J. Reigosa, J.M. Matias, E.F. Covelo, Soil Cd, Cr, Cu, Ni, Pb and Zn sorption and retention models using SVM: Variable selection and competitive model, *The Science of the total environment*, 593-594 (2017) 508-522.
- [16] T. Asadi, A. Azizi, J.-c. Lee, M. Jahani, Leaching of zinc from a lead-zinc flotation tailing sample using ferric sulphate and sulfuric acid media, *Journal of Environmental Chemical Engineering*, 5 (2017) 4769-4775.
- [17] X.W. Zhang, L.S. Yang, Y.H. Li, H.R. Li, W.Y. Wang, Q.S. Ge, Estimation of lead and zinc emissions from mineral exploitation based on characteristics of lead/zinc deposits in China, *Transactions of Nonferrous Metals Society of China*, 21 (2011) 2513-2519.
- [18] G.M. Mudd, S.M. Jowitt, T.T. Werner, The world's lead-zinc mineral resources: Scarcity, data, issues and opportunities, *Ore Geology Reviews*, 80 (2017) 1160-1190.
- [19] L.E.D. Smith, G. Siciliano, A comprehensive review of constraints to improved management of fertilizers in China and mitigation of diffuse water pollution from agriculture, *Agriculture, Ecosystems & Environment*, 209 (2015) 15-25.
- [20] Z.-r. Liu, L.-m. Zhou, P. Wei, K. Zeng, C.-x. Wen, H.-h. Lan, Competitive adsorption of heavy metal ions on peat, *Journal of China University of Mining and Technology*, 18 (2008) 255-260.
- [21] J. Wang, Q. Li, M.M. Li, T.H. Chen, Y.F. Zhou, Z.B. Yue, Competitive adsorption of heavy metal by extracellular polymeric substances (EPS) extracted from sulfate reducing bacteria, *Bioresource technology*, 163 (2014) 374-376.
- [22] P. Kampalanonwat, P. Supaphol, The Study of Competitive Adsorption of Heavy Metal Ions from Aqueous Solution by Aminated Polyacrylonitrile Nanofiber Mats, *Energy Procedia*, 56 (2014) 142-151.
- [23] Y. Dong, H. Lin, Competitive adsorption of Pb(II) and Zn(II) from aqueous solution by modified beer lees in a fixed bed column, *Process Safety and Environmental Protection*, 111 (2017) 263-269.
- [24] E. Dantas de Freitas, H. Joacy de Almeida, A. Florêncio de Almeida Neto, M.G. Adeodato Vieira, Continuous adsorption of Silver and Copper by Verde-Iodo bentonite in a fixed bed flow-through column, *Journal of Cleaner Production*, (2017).
- [25] J. Deng, Y. Liu, S. Liu, G. Zeng, X. Tan, B. Huang, X. Tang, S. Wang, Q. Hua, Z. Yan, Competitive adsorption of Pb(II), Cd(II) and Cu(II) onto chitosan-pyromellitic dianhydride modified biochar, *Journal of colloid and interface science*, 506 (2017) 355-364.
- [26] A. Pal, K. Majumder, S. Sengupta, T. Das, A. Bandyopadhyay, Adsorption of soluble Pb(II) by a photocrosslinked polysaccharide hybrid: A swelling-adsorption correlation study, *Carbohydrate polymers*, 177 (2017) 144-155.
- [27] S. Zhang, F. Xu, Y. Wang, W. Zhang, X. Peng, F. Pepe, Silica modified calcium alginate-xanthan gum hybrid bead composites for the removal and recovery of Pb(II) from aqueous solution, *Chemical Engineering Journal*, 234 (2013) 33-42.
- [28] N.E. Mousa, C.M. Simonescu, R.-E. Pătescu, C. Onose, C. Tardei, D.C. Culiță, O. Oprea, D. Patroi, V. Lavric, Pb<sup>2+</sup> removal from aqueous synthetic solutions by calcium alginate and chitosan coated calcium alginate, *Reactive and Functional Polymers*, 109 (2016) 137-150.
- [29] L. De Pablo, M.L. Chávez, M. Abatal, Adsorption of heavy metals in acid to alkaline environments by montmorillonite and Ca-montmorillonite, *Chemical Engineering Journal*, 171 (2011) 1276-1286.
- [30] M. Ferhat, S. Kadouche, N. Drouiche, K. Messaoudi, B. Messaoudi, H. Lounici, Competitive adsorption of toxic metals on bentonite and use of chitosan as flocculent coagulant to speed up the settling of generated clay suspensions, *Chemosphere*, 165 (2016) 87-93.

- [31] P. Tan, Y. Hu, Q. Bi, Competitive adsorption of Cu<sup>2+</sup>, Cd<sup>2+</sup> and Ni<sup>2+</sup> from an aqueous solution on graphene oxide membranes, *Colloids and Surfaces A: Physicochemical and Engineering Aspects*, 509 (2016) 56-64.
- [32] M. Talebi Atouei, R. Rahnemaie, E. Goli Kalanpa, M.H. Davoodi, Competitive adsorption of magnesium and calcium with phosphate at the goethite water interface: Kinetics, equilibrium and CD-MUSIC modeling, *Chemical Geology*, 437 (2016) 19-29.
- [33] L.E. Hernández-Hernández, A. Bonilla-Petriciolet, D.I. Mendoza-Castillo, H.E. Reynel-Ávila, Antagonistic binary adsorption of heavy metals using stratified bone char columns, *Journal of Molecular Liquids*, 241 (2017) 334-346.
- [34] M.L. Soto, A. Moure, H. Domínguez, J.C. Parajó, Batch and fixed bed column studies on phenolic adsorption from wine vinasses by polymeric resins, *Journal of Food Engineering*, 209 (2017) 52-60.